

iDynoMiCS: next-generation individual-based modelling of biofilms

Laurent A. Lardon,^{1,2†} Brian V. Merkey,^{1,3†}
Sónia Martins,⁴ Andreas Dötsch,⁵
Cristian Picioreanu,⁶ Jan-Ulrich Kreft⁴ and
Barth F. Smets^{1*}

¹Department of Environmental Engineering, Technical University of Denmark, Bygningstorvet 115, 2800 Kgs. Lyngby, Denmark.

²Laboratory of Environmental Biotechnology, INRA, Avenue des étangs, 11100 Narbonne, France.

³Department of Engineering Sciences and Applied Mathematics, Northwestern University, 2145 Sheridan Road, Evanston, IL 60201, USA.

⁴Centre for Systems Biology, School of Biosciences, The University of Birmingham, Edgbaston, Birmingham B15 2TT, UK.

⁵Chronic Pseudomonas Infections Group, Helmholtz Centre for Infection Research, Inhoffenstrasse 7, D-38124 Braunschweig, Germany.

⁶Department of Biotechnology, Delft University of Technology, Julianalaan 67, 2628 BC Delft, The Netherlands.

Summary

Individual-based modelling of biofilms accounts for the fact that individual organisms of the same species may well be in a different physiological state as a result of environmental gradients, lag times in responding to change, or noise in gene expression, which we have become increasingly aware of with the advent of single-cell microbiology. But progress in developing and using individual-based modelling has been hampered by different groups writing their own code and the lack of an available standard model. We therefore set out to merge most features of previous models and incorporate various improvements in order to provide a common basis for further developments. Four improvements stand out: the biofilm pressure field allows for shrinking or consolidating biofilms; the continuous-in-time extracellular polymeric substances excretion leads to more realistic fluid behaviour of the extracellular matrix, avoiding

artefacts; the stochastic chemostat mode allows comparison of spatially uniform and heterogeneous systems; and the separation of growth kinetics from the individual cell allows condition-dependent switching of metabolism. As an illustration of the model's use, we used the latter feature to study how environmentally fluctuating oxygen availability affects the diversity and composition of a community of denitrifying bacteria that induce the denitrification pathway under anoxic or low oxygen conditions. We tested the hypothesis that the existence of these diverse strategies of denitrification can be explained solely by assuming that faster response incurs higher costs. We found that if the ability to switch metabolic pathways quickly incurs no costs the fastest responder is always the best. However, if there is a trade-off where faster switching incurs higher costs, then there is a strategy with optimal response time for any frequency of environmental fluctuations, suggesting that different types of denitrifying strategies win in different environments. In a single environment, biodiversity of denitrifiers is higher in biofilms than chemostats, higher with than without costs and higher at intermediate frequency of change. The highly modular nature of the new computational model made this case study straightforward to implement, and reflects the sort of novel studies that can easily be executed with the new model.

Introduction

Surfaces in most environments are rapidly colonized by bacteria that form biofilms: aggregates of cells and abiotic particulates within an organic polymeric matrix of microbial origin (Characklis and Marshall, 1990). A vast array of observational techniques has become available to study the microbial, chemical and physical properties of biofilms at increasingly refined spatial and temporal resolution (Lawrence *et al.*, 1991; Bishop and Yu, 1999; Heydorn *et al.*, 2000; Xavier *et al.*, 2003). These tools indicate that biofilms are highly structured systems, with an organization, function, shape and composition that are strongly related to the applied environmental conditions (Watnick and Kolter, 2000; Stoodley *et al.*, 2002).

These observational advances have been matched by a refinement in mathematical or computational

Received 8 June, 2010; accepted 1 December, 2010. *For correspondence. E-mail b fsm@env.dtu.dk; Tel. +45 4525 2230; Fax +45 4593 2850. †These authors contributed equally to this work.

descriptions of biofilms (Hellweger and Bucci, 2008). Computational biofilm models must jointly consider the fast processes affecting solutes (reaction and transport by diffusion or convection) and the slower processes affecting bacterial mass (growth and division, transport within the biofilm, detachment or erosion at the biofilm surface, and attachment to the surface). These processes obey mass conservation and for a continuum space are typically written as partial differential equations (PDEs), which can be solved using standard numerical methods. Biofilm models initially represented biomass as a continuum, based on population-averaged behaviour of different functional groups. Biofilm models have since progressed from simpler steady-state one-dimensional (1D) models to more complex time-dependent 1D models (Wanner and Gujer, 1986; Wanner and Reichert, 1996), with further expansion to two- and three-dimensional (2D and 3D) models (Dockery and Klapper, 2001; Eberl *et al.*, 2001; Laspidou and Rittmann, 2004a; Wanner *et al.*, 2006; Alpkvist and Klapper, 2007b; Duddu *et al.*, 2009; Merkey *et al.*, 2009). It has been observed, though, that locally constrained environments may cause individual or localized behaviours to vary significantly from population-averaged behaviour (Hellweger and Bucci, 2008; Stewart and Franklin, 2008). In addition, within the high microbial density of a biofilm there exists a significant diversity within functional groups that is potentially exacerbated by the large solute gradients common to such systems. This diversity causes very localized dominance or colocalization of specific species (Picioreanu *et al.*, 2004b; Batstone *et al.*, 2006; Matsumoto *et al.*, 2007a; Downing and Nerenberg, 2008), and allows even minority species to survive (Boles *et al.*, 2004); such local observations of biofilm composition are not adequately described or predicted by population-averaged models. A wide interest to develop alternative approaches that capture these cell-level and micro-scale differences, as well as a desire to understand how individual processes, interactions and variability affect the macroscopic structure of biofilms, has led to the development of individual-based models (IbMs) for microbial biofilms.

In an IbM individuals or agents are modelled explicitly, with the higher-level population behaviour emerging from their low-level interactions. In IbMs, individuals are unique and discrete entities that differ in one or more properties such as position, biomass composition and metabolic behaviour (Hellweger and Bucci, 2008). The first true IbM for microbial biofilms (BacSim) was introduced and subsequently improved by Kreft and colleagues (1998; 2001). Further work added extracellular polymeric substances (EPS) to the model (Kreft and Wimpenny, 2001), with EPS formation stoichiometrically coupled to growth; formed EPS was bound first to the bacterial agent, but could then

be excreted as a separate agent that would subsequently engage in shoving along with the bacterial agents. An alternative method to treat EPS was introduced by Alpkvist and colleagues (2006), who used a continuum representation of EPS to capture the incompressible, viscous fluid nature of EPS (Klapper *et al.*, 2002), combined with an IbM of microbial cells. It has been found that the inclusion of EPS, by either method, has a large effect on the dynamics of biofilm growth. Xavier *et al.* previously made important improvements to the IbM approach by introducing a more advanced detachment method and by allowing each agent to contain multiple components (e.g. active and inactive biomass, storage polymers, polyhydroxy-alkanoates, glycogen), each of which could undergo various specified bioconversions (Xavier *et al.*, 2005a,b). IbMs have been used also to model biofilms using individual agents to represent not individual cells but rather clusters of cells of the same type (Picioreanu *et al.*, 2004a).

Outcomes emerging from these IbMs have predicted several structural features of microbial biofilms that seem to match experimental observations: the predominantly clonal growth of microbes in biofilms (multiplication of immobilized cells leads to clusters of isogenic cells or clonal microcolonies) (Kreft *et al.*, 2001); the shape and location of microcolonies of interacting community members (Picioreanu *et al.*, 2004b; Alpkvist *et al.*, 2006; Batstone *et al.*, 2006); and the temporal consolidation of biofilms with depth (Alpkvist *et al.*, 2006). IbMs have also been used to test several evolutionary and ecological hypotheses: Kreft (2004) explored how elementary altruistic behaviour (increasing economy of resource use [growth yield] at the cost of growth rate) can emerge and be maintained in biofilms but not in suspended growth cultures, while Xavier and Foster (2007) looked at the strong evolutionary advantages that EPS producers have in mixed genotype biofilms. In addition, IbMs have confirmed and provided several mechanistic explanations for phenomena such as biofilm fingering (Kreft *et al.*, 2001), the surprising location of initial biofilm growth in square-channel monolith reactors (Ebrahimi *et al.*, 2005), the long-term survival of slow growers in deeper portions of a biofilm (Picioreanu *et al.*, 2004a), and the effect of microbial motility on biofilm morphology (Picioreanu *et al.*, 2007; Mabrouk *et al.*, 2010). IbMs have also been successfully applied to describe and optimize various biofilm and granular reactor applications (Picioreanu *et al.*, 2005; Xavier *et al.*, 2005a; 2007; Batstone *et al.*, 2006; Matsumoto *et al.*, 2007a; Matsumoto *et al.*, 2010), and biofilm control strategies based on the disruption of the EPS matrix have also been investigated (Xavier *et al.*, 2005c).

In spite of the general maturity of biofilm modelling approaches, IbMs have, so far, not seen general use like

the 1D continuum model by Wanner and Gujer (1986), which is widely available through the Aquasim software package (Reichert, 1994). In order to address this gap, we present here a new modelling platform specifically dedicated to individual-based modelling of microbial communities, meant to improve accessibility to non-programmers and to provide a backbone for future developments proposed by any interested contributor. iDynoMiCS (standing for individual-based Dynamics of Microbial Communities Simulator) is built on the foundation of earlier models (Kreft *et al.*, 2001; Kreft and Wimpenny, 2001; Picioreanu *et al.*, 2004b; Xavier *et al.*, 2005a,b), and is open-source software developed under a CeCILL license (<http://www.cecill.info/index.en.html>). Details about how to obtain iDynoMiCS from the website <http://www.idynamics.org> are contained in the *Supporting information*. The iDynoMiCS model also includes improvements to the IbM approach, which we describe in depth in this manuscript.

Similarly to former individual-based biofilm models, iDynoMiCS is meant to be used to answer microbial ecology questions by the use of simulations resolved at the micro-organism or microcolony scale; it also exhibits interactions between global dynamics (e.g. concentrations in the free liquid phase) and individual heterogeneity or spatial structures. Also like previous IbMs of biofilms, iDynoMiCS may not necessarily be the right tool to answer other questions (Wanner *et al.*, 2006), such as predicting colonization resistance in the gut microbiota as a whole (Freter *et al.*, 1983) or studying the efficacy of particular wastewater reactor configurations (Reichert, 1994). iDynoMiCS is also, like other IbMs, more complex and computationally demanding than simpler biofilm models (Reichert, 1994; Rittmann and McCarty, 2001), and this cost should be considered as one evaluates whether to use iDynoMiCS. In addition, many features important to particular systems (e.g. modelling electric fields or chemical reactions occurring separately from bacterial agents) are not yet included in iDynoMiCS, but iDynoMiCS was designed to allow such capabilities to be easily added.

As a whole though, the improvements to IbMs introduced with iDynoMiCS allow new types of studies to be made, and allow such studies to be made by non-programmers much more easily. To illustrate how the new features of the iDynoMiCS model extend the range of problems addressable using an IbM, we will use the model to study denitrifying communities exposed to varying conditions. Many studies have shown that some denitrifiers switch on denitrification pathways rapidly once oxygen becomes depleted, while others switch on only slowly, and others still do not switch off at all under aerobic conditions (Robertson and Kuenen, 1984; Körner and Zumft, 1989; Kucera *et al.*, 1990; Ye *et al.*, 1995; Baumann *et al.*, 1996; Otte *et al.*, 1996). Here we use iDynoMiCS to show that the observed variety of denitrify-

ing strategies can be explained by assuming that the cost of switching between aerobic and anaerobic growth modes increases with the rate of switching.

In a companion paper (Merkey *et al.*, 2011), we use an extension of the basic model to explore the spread of mobile genetic elements in biofilms.

Model description

In recognition of the difficulties posed in describing and reviewing IbMs, Grimm *et al.* proposed the Overview, Design concepts and Details (ODD) format for describing IbMs to ensure consistently structured, complete and comparable descriptions (Grimm *et al.*, 2006). We therefore follow the ODD concept. Further details are available in the *Supporting information* for some parts of the model description.

Purpose

The purpose of iDynoMiCS is to simulate the growth of populations and communities of individual microbes (small unicellular organisms such as bacteria, archaea and protists) that compete for space and resources in biofilms immersed in aquatic environments. With iDynoMiCS we seek to understand how individual microbial dynamics lead to emergent population- or biofilm-level properties and behaviours. iDynoMiCS also allows simulation of a well-mixed unstructured chemostat environment to evaluate the effect of spatial structure on growth dynamics.

Scale and state variables

The fundamental agent in iDynoMiCS is the individual microbe, characterized by state variables including: location, size, density, relative composition (active biomass, inert biomass, EPS), species type, catalysed reactions and associated rate and stoichiometric coefficients, and genealogy. iDynoMiCS also includes particulate EPS agents that are produced by microbes through an excretion process and characterized by their species of origin, position, size and density. Individual agents interact directly mechanically through shoving in the competition for space. While the agents comprise the lowest hierarchical level in the iDynoMiCS structure, they are the entities that mediate, through growth and related processes, the dynamics of the entire system.

Agents that share certain characteristics or parameters (such as reaction types) are grouped into species, but this grouping is purely organizational. The agent population as a whole, though, is treated as a collective (see *Design concepts*) to ensure that all agents take part in the purely mechanical interactions leading to biomass spreading

and detachment. The spatial extent of this cluster of agents defines the region that is considered to be part of the biofilm structure, with the region outside the biofilm considered to be liquid.

Computational constraints limit simulations to a computational domain that is a small subset of the macro-scale world, currently on the order of several hundred to several thousand microns in extent in each spatial dimension. All simulated agents must reside somewhere within the computational domain, and by default are restricted to the biofilm (a region that is a subset of the computational domain). Within the domain, solutes are represented by concentration fields that vary in space and time because of mass transport (diffusion and advection) dynamics and the reactions by which they are affected. Included in the model can be a representation of the well-mixed macro-scale liquid volume within which the biofilm community is immersed (e.g. to simulate a biofilm in an ideally mixed reactor), called the bulk compartment. The computational domain is often connected to at least one such ideally mixed compartment. The bulk compartment may be affected by reactions and mass transfer exchange with the biofilm and with the external environment through hydraulics, and bulk solute concentrations may thereby vary in time. Physical interaction of the bulk liquid volume with the biofilm structure in the form of shear or erosion forces will lead to detachment of microbes from the biofilm, and this process is included as well.

In addition to the solute dynamics of the bulk, it is possible to simulate the fate of free microorganisms and hence to study a well-mixed, unstructured chemostat. For this purpose, a stochastic chemostat is defined by populating a homogeneous spatial domain with microorganisms. In chemostat simulations, most spatial properties of agents, solutes and the computational domain are excluded: agent locations are ignored; solute concentrations do not vary spatially in the domain and are fixed at the current bulk compartment value; all agents experience the same bulk concentrations for solutes; and the only physical interaction of agents with the world is through a

stochastic dilution process that removes a certain number of randomly chosen discrete cells from the system during each timestep.

The overall properties of the computational domain, the bulk compartment(s) and the erosion forces are grouped into a 'world' descriptor, which emphasizes the interplay between the micro- and macro-scale environments captured by iDynoMiCS and other IbMs.

Process overview and scheduling

During a single global timestep, the dynamics of the solute concentration fields, the bulk compartment and the agents are applied independently, although the dynamics of each depend on the current state of the others (Algorithm 1). Addressing each class of dynamics separately is possible because they all operate on different timescales (Picioreanu *et al.*, 1999). In addition, the dynamics of the agents are further broken down into smaller timesteps to account for the varied processes affecting agent growth, division and movement, as well as any additional processes an agent may carry out. Once these steps are completed, erosion effects are applied to the biofilm structure as a whole, the global time is incremented, and the next timestep taken.

Design concepts

The iDynoMiCS structure considers several important ecological concepts in model design and in the interpretation of model outputs.

Emergence. The biofilm structure and composition emerge from the activity of individual agents, whose behaviours depend on the solute concentration fields, the behaviour of neighbouring agents, and the erosion or shear forces acting on the biofilm.

Adaptation. Unlike previous biofilm models, in iDynoMiCS biochemical growth reactions are uncoupled from

Algorithm 1. Pseudo-code describing one global timestep iteration of the individual-based simulator.

-
- 1 Solve solute mass balances in the computational domain for the given agent distribution and bulk solute concentrations; this sets the solute concentration fields
 - 2 Update bulk concentrations based on new solute concentration fields
 - 3 While agent timestep < global timestep
 - a. Perform any actions specific to a particular species or agent type
 - b. Compute growth, decay and division or death of agents to update agent size and mass, and add or remove agents if needed
 - c. Compute pressure field and apply pressure-driven movements to agents
 - d. Apply shoving and spring relaxation to update agent locations
 - 4 Apply detachment of agents by erosion and remove disconnected parts of the biofilm
 - 5 Update global timestep
-

When a chemostat is being simulated, step 1 is simplified due to the spatial homogeneity but the time resolution is increased, steps 2, 3c, and 3d are skipped, and step 4 is replaced by stochastic agent dilution.

species, allowing individuals of a species to carry out different sets of reactions. This makes it possible to simulate agents that adapt their metabolic reactions to environmental conditions.

Fitness. This is an emergent property included implicitly as a function of an agent's growth properties.

Prediction. iDynoMiCS is able to predict biofilm structure and composition, as well as time-varying solute concentrations in the bulk compartment and in the biofilm. While the abstract agents in iDynoMiCS are not meant to predict the behaviour of individual real-life microbial agents, the simulation as a whole is able to predict the response of a bacterial population to its environment.

Sensing. Individual agents grow based on implicit sensing of local solute concentrations and sensing of the environment can lead to changes in behaviour and metabolism.

Interaction. The agents, bulk compartment and solute concentration state variables interact with one another through reactions, and agents also interact mechanically with one another by shoving for space during growth and EPS excretion.

Stochasticity. The stochastic processes in iDynoMiCS include: (i) the initial agent locations are randomly chosen within a particular rectangular region, unless the user specifies a list of agents with initial positions, (ii) the initial agent masses are randomly chosen around an average value, unless specified directly by the user, (iii) the cell division threshold volume is chosen randomly around an average division size, (iv) the cell death threshold volume is chosen randomly around an average death size, (v) upon cell division, daughter cell sizes are chosen stochastically around equally sized daughter cells, (vi) also upon cell division, daughter cells are positioned with zero overlap and equidistant from the mother cell's centre, but are oriented in a random direction (Fig. S2), (vii) EPS excretion in the form of new particles occurs in a randomly chosen direction and (viii) the order in which agents are updated during a single global timestep is made random during each step. For investigating the importance of stochasticity, processes (i) to (v) can be made deterministic, and time series of population densities in simulations with stochasticity at a minimum are typically indistinguishable. For processes (vi) and (vii) there is no unique deterministic solution.

Collectives. Only the biofilm community as a whole is tracked explicitly, in order to allow any processes that depend on the biofilm surface, such as erosion and

detachment, to be treated correctly. All agents are organized into lists to ensure each agent is processed exactly once per timestep. Individuals are also grouped by metabolic type (guilds) for calculation of reaction rates and solute fluxes or grouped according to processes they have in common, but this is only for efficiency and does not imbue these organizational units with any additional properties. In addition, guild membership is not permanent and can be modified at any moment for any individual according to its own strategy and perceptions.

Observation. At specified intervals iDynoMiCS stores the solute concentration fields and the state of each agent (species, location, masses of all compartments, composition, genealogy, growth rate, etc.). The latter information can also be read in as initial condition in order to start a new simulation based on a previous run.

Initialization

Initialization in iDynoMiCS is under user control. The size and boundaries of the computational domain and the dynamics of the bulk compartment should be based on the physical system being studied. The user must specify species types and reactions included in the model. The agent initial conditions include setting initial values for agent state variables, and setting the initial number of and inoculation region for the agents. Agents may be defined stochastically within conditions specified by the user, or precise initial conditions can be specified with an input file. Solute concentration fields do not need to be specified because the steady-state solute concentrations can be calculated from the boundary conditions and distribution of agents with their reaction rates.

Input

The inputs to iDynoMiCS, meaning the imposed dynamics corresponding to the real-world system being studied, consist of defining the dynamics of the bulk compartment (constant or time-varying, and for the latter case including influent concentrations and dilution rates), specifying the erosion strength (a function of macro-scale environmental stresses), possibly imposing a maximum biofilm thickness, and setting the mass transfer resistance to the biofilm by setting the thickness of the diffusion boundary layer.

Submodels

Here we describe in detail each of the components of iDynoMiCS. For many submodels further details are available in the *Supporting information*.

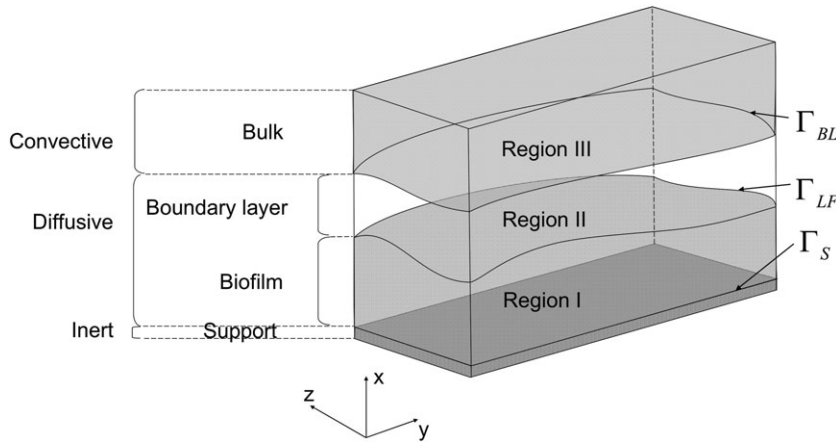


Fig. 1. The computational domain including the support as an external boundary. Region I represents the biofilm, Region II the diffusion boundary layer and Region III the well-mixed bulk compartment. While the choice of the orientation of the axes x , y and z is not conventional, it preserves the existence and location of x and y axes when reducing the model from 3D to 2D.

The computational domain. The computational domain is an evenly spaced rectilinear grid described by its dimensionality (2D or 3D), its size, its geometry and the behaviour at its boundaries. Within the computational domain several regions are defined, as illustrated in Fig. 1: the support is the surface to which agents can adhere; the bulk compartment (Region III) represents the well-mixed bulk liquid within which the computational domain is immersed, and within this region solute concentrations are fixed to their bulk values; the biofilm matrix (Region I) is composed of microbial cells embedded in a viscous medium produced by the microbes (extracellular polymeric substances, EPS); and the diffusion boundary layer (Region II) is a purely diffusive liquid compartment at the interface between the bulk compartment and the biofilm. In Regions I and II, the solute concentration fields vary in space because of diffusion and reaction dynamics, and, because these processes are much faster compared with the timescale of agent growth, solute concentrations are assumed at all times to be in pseudo steady-state compared with agent dynamics (Picioreanu *et al.*, 1999). In Region III, the solute concentration fields are kept equal to the concentration in the world-level bulk compartment, and, through diffusive interactions with Regions I and II, Region III connects the micro-scale agents with the macro-scale bulk compartment. The conditions at the domain boundaries (4 in 2D and 6 in 3D) affect the behaviour of the model for the agents (Fig. S1) and the solutes, and, although iDynoMiCS may be extended to use any boundary type, the current implementation includes a default set of boundary types: no-flux, constant or variable concentration, solute-permeable membrane, and periodic boundaries (see *Supporting information*).

Solute species dynamics. Solute dynamics in the biofilm and boundary layer are affected by two processes (Fickian diffusion and agent-mediated reactions), and, as in previous models [see the timescale discussion in

Picioreanu *et al.* (2001)], we assume that the solute fields are in pseudo steady-state with respect to biomass growth. Therefore at each step we solve the following elliptic PDE:

$$\nabla \cdot (D_s(\vec{x}) \cdot \nabla S(\vec{x})) + r_s(\vec{x}) = 0. \quad (\text{III-1})$$

Here \vec{x} is the position vector, $D_s(\vec{x})$ is the local solute diffusion coefficient, $r_s(\vec{x})$ is the local solute reaction rate, and ∇ can be read as the gradient of a field (i.e. is the vector gradient operator $\nabla = \hat{i} \frac{\partial}{\partial x} + \hat{j} \frac{\partial}{\partial y} + \hat{k} \frac{\partial}{\partial z}$). The diffusion coefficient and reaction rates in this equation take different forms for different regions: reaction rates in the biomass-free boundary layer are zero, and the effective diffusion coefficient is decreased within the biofilm compared with the liquid value (the effective diffusivity is typically 0.8 times the coefficient in water) in order to account for the increased mass transfer resistance (Rittmann and Manem, 1992; Stewart, 2003). The solute concentration fields described by the elliptic PDE in (Eq. III-1) are solved using an efficient multigrid method (Brandt, 1977; Picioreanu *et al.*, 2004a; Xavier *et al.*, 2005a), and the flexible, modular structure of iDynoMiCS facilitates implementation of additional solvers.

A dynamic bulk compartment varies in time due to inflow, outflow and reactions. Ignoring any reactions occurring in the bulk compartment and including only reactions in the biofilm, we may write a mass balance on the bulk compartment:

$$\frac{dS_B}{dt} = D \cdot (S_{in} - S_B) + R_S \cdot \sigma_R. \quad (\text{III-2})$$

Here S_B is the solute concentration in the bulk compartment, D the dilution rate of the bulk compartment, S_{in} the influent solute concentration, σ_R the specific surface area of the bulk compartment (total area of carrier surface in the bulk divided by bulk compartment volume) and R_S the net reaction rate per carrier area. For modelling systems

where oxygen (or solute) concentrations are not affected by the liquid dilution rate, the iDynoMiCS dynamic bulk routines also allow for setting constant concentrations for single solutes.

Agent representation as particles. Agents are represented by incompressible (hard) spheres (in 3D simulations) or cylinders (in 2D simulations). In the default implementation two types of agents are included: bacterial agents and free EPS particles. However, because microbial systems may involve interactions not only between bacterial cells, but also with archaea, protozoa, algae or fungi, iDynoMiCS allows for the introduction of non-bacterial agents. By default, iDynoMiCS assumes a strict correspondence between individual agent and cell. All agents are characterized by particular state variables (see *Scale and state variables*). In addition, microbial agents but not EPS particles can be structured with compartments (by default active biomass, inert biomass, capsular or bound EPS). The agent structure includes an inner 'cell' consisting of all intracellular components (active and inactive biomass, storage compounds, etc.) along with an outer layer that consists of the capsular EPS. Each compartment requires a density ρ_i , and the mass m_j and volume V_j^{total} of an individual j are calculated making use of the distinction between the cell and capsular EPS:

$$m_j = \sum_{i \in cell} m_{i,j} + \sum_{i \in capsule} m_{i,j} \quad (III-3)$$

$$V_j^{total} = V_j^{cell} + V_j^{capsule} = \sum_{i \in cell} \frac{m_{i,j}}{\rho_i} + \sum_{i \in capsule} \frac{m_{i,j}}{\rho_i}$$

The radii of the inner cell and entire agent are calculated using the volumes V_j^{cell} and V_j^{total} respectively.

During a single global timestep, all agents in a simulation are updated in a random order, with the order changed for each step; this randomization removes any bias that may arise because of the order of updating. An agent update may affect agent properties such as size, composition or position, along with any properties specific to a particular agent type (e.g. enabling or disabling a reaction in response to local conditions). Even though some agent properties may not change during an update, the simulator does not skip any agents during the update step.

Cellular growth. In contrast to previous biofilm lbMs, agent-mediated biochemical reactions here are defined independently of the species, so that an individual agent may carry out a different suite of reactions than other individuals of the same species. The metabolic switching case study described in *Case study: metabolic switching for denitrification in fluctuating environments* is an example where this modelling capability is useful. Reac-

tion descriptions are based on the commonly used matrix format (Wanner and Gujer, 1986; Henze, 2000; Xavier *et al.*, 2005a). Each reaction has an overall rate expression r_i that is used to describe how a reaction affects solute and particulate components by means of a yield coefficient Y_i ; the net reaction rate for a component j is then found by summing all the reactions by which it is affected:

$$r_{j,Net} = \sum_{i \in \substack{\text{involved} \\ \text{reactions}}} Y_{i,j} \cdot r_i \quad (III-4)$$

Reactions respect mass conservation principles, and negative stoichiometric coefficients indicate consumption while positive coefficients indicate production. The reaction rate r_i is usually defined by the product of different kinetic factors representing saturation and/or inhibition by a compound (e.g. Monod/Michaelis-Menten or Haldane kinetics). The reaction rate is also proportional to the mass of the catalysing compartment, so that an individual agent may catalyse several reactions simultaneously, each by a specific compartment.

Cell division and death. Agents grow and shrink because of their metabolism, but agent sizes are restricted to a particular window: cell division or death occurs instantaneously when an agent reaches a user-defined threshold radius. To avoid artificial synchronization of agent divisions, the decision to divide or die does not occur exactly at the threshold; instead the decisions are based on test radii taken from Gaussian distributions of the user-specified threshold radii using Coefficients of Variation of, by default, 10%, with the distributions cut off outside two standard deviations.

During division the agent's mass is split more or less evenly between its daughters, chosen via a Gaussian distribution that by default gives equal volumes for the daughter cells with a 10% Coefficient of Variation and cut off outside two standard deviations. The orientation of the division direction is randomly chosen and daughter agents are positioned with zero overlap (Fig. S3), with any neighbour overlap addressed through shoving (see *Mechanical interactions*).

Agent death is included as a way to remove small, inactive agents from the simulation. Agents that shrink below a death-size threshold are removed from the simulation, and so long as the death size is chosen to be sufficiently small (e.g. on the order of 0.1 μm) the impact on overall simulation mass balance is negligible. For simulations where a small death radius is not appropriate, the mass loss due to removal of larger agents would no longer be insignificant, and in that case an alternative to this simple approach would be to include a lysis reaction that converts dying cell mass into soluble COD.

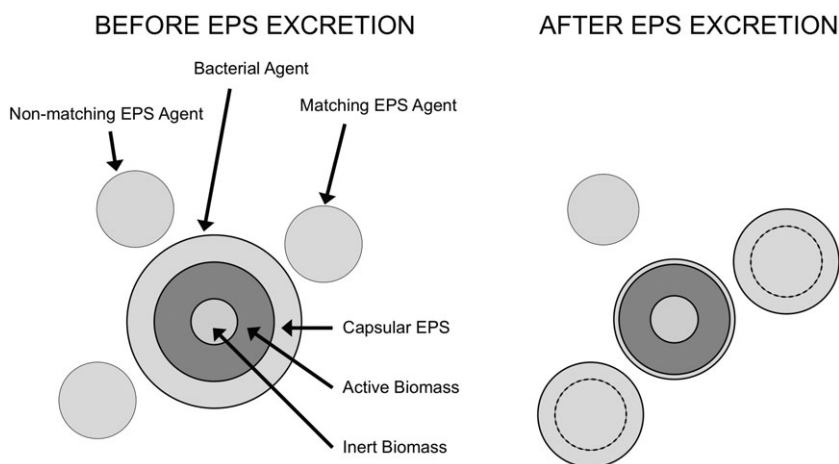


Fig. 2. EPS capsule excretion via continuous transfer to neighbouring EPS particles. When EPS is excreted by an agent, the excreted EPS is shared among any neighbouring EPS agents of the same type. In the case when no such agents are present, a new EPS particle will be created.

EPS excretion. The EPS matrix surrounding cells in the biofilm has been previously represented via both particulate and continuum methods, and iDynoMiCS introduces two improvements to the particulate representation of EPS proposed in Kreft and Wimpenny (2001). First, EPS accumulated in an extracellular compartment by EPS-producing agents is continuously transferred to the environment (i.e. during each timestep), rather than being released only during discrete events (i.e. only during some timesteps). As illustrated in Fig. 2, during an agent step the agent's neighbourhood is scanned to find all EPS particles of the same type within a certain radius, and the released EPS is distributed evenly between them; if no such agents are found, a new EPS particle is created. A consequence of this approach is the decoupling of the kinetics of production and transfer of EPS, allowing release of matrix EPS even in the absence of microbial growth. The second improvement over previous particulate EPS treatments is in the size of EPS particulates used by iDynoMiCS. Following smoothed particle hydrodynamic methods (Gingold and Monaghan, 1977), we impose smaller radii for EPS particulates, an approach that appears to recreate a viscous fluidic biofilm matrix (Klapper *et al.*, 2002). To our knowledge no previous model has used small EPS spheres as an alternative to the continuum treatment in Alpkvist and colleagues (2006). Representing EPS as particles allows tracking of the origin of the EPS particles and to simulate different types of matrix compounds, such as DNA or proteins that are possibly produced by different species.

Mechanical interactions. Agent growth, division, shrinking and death are the source of agent movement within the biofilm. iDynoMiCS combines a finer- with a coarser-scale mechanism for capturing these sources of movement and for moving agents to account for these processes: agent shoving, and biomass growth pressure.

At the local level, agent overlaps are avoided through a relaxation algorithm that determines the steady-state agent locations with the minimal number of overlaps (Algorithm S1). Any pair-wise agent overlap resulting from agent growth or division is resolved by moving each agent apart by half the overlap distance (Fig. S4); to avoid any bias, the algorithm first sums all movement vectors due to the current configuration and then applies all agent movements at once, continuing the cycle until the number of agents still moving is negligible (at the typical parameter setting, less than 5% of the total number of agents). Previous lbMs of biofilms have used such shoving algorithms effectively to model growing biofilms (Kreft *et al.*, 2001). Further details of the shoving algorithm are provided in the *Supporting information*.

At the global level, inclusion of a biomass growth pressure addresses sources of agent movement that are not captured through agent shoving, such as biomass consolidation as a result of decay, cell lysis or hydrolysis of EPS (either bound or free) deep in a biofilm (Laspidou and Rittmann, 2004b). lbMs that include only agent shoving work well for modelling expanding biofilms, but will not capture the negative pressure of consolidation that acts to pull biomass closer together, thereby shrinking the biofilm. Biofilm-scale advective motion of biomass may be addressed by applying a mass balance on each grid element that takes account of the effects of growth and decay of biomass as well as this advective motion of biomass. These growth and decay processes contribute to a biomass pressure P , as defined previously by Klapper and colleagues (2002) and Alpkvist and colleagues (2006), and this pressure is alleviated through the advective movement of biomass. Advection within the biofilm is described by Darcy's law, where the advective velocity \vec{u} is given by: $\vec{u} = -\lambda \nabla P$, with λ [units ($\text{m}^3 \text{s kg}^{-1}$)] a material property called the Darcy parameter that is inversely proportional to the material's dynamic viscosity. In practice, the Darcy parameter ends up cancelling out

during the computation of the resulting biomass velocity (Alpkvist *et al.*, 2006), and for this reason λ is often set to 1 to simplify computation. Following Alpkvist and colleagues (2006), application of mass conservation for each grid element in the biofilm yields the following elliptic equation for the pressure P :

$$\nabla \cdot (-\lambda \nabla P) + \sum_{j \in \text{elements}} \frac{r_j}{\rho_j} = 0 \quad (\text{III-5})$$

where r_j and ρ_j are the mass production rate and density of agent j , respectively, and the ratio gives the rate of volume production. The boundary conditions for calculating the pressure field P include a no-flux boundary at the substratum and any periodicity in the lateral directions following the solutes, along with an imposed pressure $P = 0$ outside the biofilm. These boundary conditions allow for calculation of the pressure P via (Eq. III-5), and the local advective velocity may be computed by application of Darcy's law. The resulting local advective velocity is applied to each agent by adding it to other movement terms caused by shoving, cell division and EPS particle excretion. In the case of high pressure gradients, a smaller timestep will be imposed on agent movement in order to maintain numerical stability.

Because growth of cells leads to an increase in the local pressure as well as to overlap of neighbours, the two mechanisms are consistent. Therefore, the biomass pressure is also used to move agents as a result of biomass growth because it tends to be more efficient than shoving algorithms for larger-scale redistribution of biomass (Dockery and Klapper, 2001; Alpkvist *et al.*, 2006). However, although the pressure field can capture movement as a result of growth, it cannot replace agent shoving because the biomass pressure field is too coarse to resolve overlaps between neighbours.

During a simulation, the biomass pressure computation and resulting agent movement are carried out before agent shoving so that the latter may address any overlap introduced during the pressure movement step (Algorithm 1).

Erosion. Some previous models have used the Navier-Stokes equations and visco-elastic properties of biofilms to model shear and erosion of a biofilm surface mechanistically (Picioreanu *et al.*, 2001; Alpkvist and Klapper, 2007a; Duddu *et al.*, 2009). However, this treatment introduces computational complexities, necessitates smaller timescales (on the order of seconds), and relies on parameters that are difficult to measure. iDynoMiCS is meant to model a longer timescale and consequently uses a more global erosion effect: as in Xavier and colleagues (2005b), an erosion speed function, F_{Det} , is defined at each point on the biofilm-liquid interface and is used to remove biomass continuously at each timestep (Fig. S5). Erosion may sometimes cause separation of

portions of the biofilm from the substratum; these detached portions are found by a process of connected volume filtration and removed from the computational domain (Xavier *et al.*, 2005b). Further details of this process are available in the *Supporting information*.

Individual-based chemostat. iDynoMiCS is also suitable for the simulation of bacterial growth and their interactions in an unstructured environment, such as a chemostat. When simulating this type of environment, we ignore the spatial position of the cells and skip position-related steps during agent updates (Algorithm 1). The concentrations of the solutes in a chemostat are spatially invariant, and are simply the balance between the processes of inflow, outflow and consumption as a result of bacterial growth. Solute dynamics are calculated using an ordinary differential equation (ODE) solver adapted from linearly implicit formulas for stiff systems based on Rosenbrock methods (Gear, 1971; Shampine, 1982; Shampine and Reichelt, 1997). With an individual-based chemostat, dilution of cells is stochastic, meaning that the number of agents to be washed out per timestep is computed from the set dilution rate, but that the individuals to be washed out are randomly chosen from all agents, including EPS. In addition, individuals might be in different physiological states despite the uniform environment [e.g. because of noise in gene expression (Kaern *et al.*, 2005) or specific cell morphologies (Balagaddé *et al.*, 2005)], and it is possible to simulate and track direct interactions between individuals.

Results and discussion

Validation of iDynoMiCS against benchmark problem BM3

iDynoMiCS has been validated against the 2D multi-species biofilm benchmark BM3 proposed by the International Water Association task group on biofilm modelling (Noguera and Picioreanu, 2004; Rittmann *et al.*, 2004; Wanner *et al.*, 2006). In most cases there is good agreement of the output of iDynoMiCS with various previous models (Table S5) (Noguera and Picioreanu, 2004). However, iDynoMiCS results are significantly different from previous models in one of the BM3 comparison cases, a case that was particularly sensitive to model peculiarities (Noguera and Picioreanu, 2004). From this and other validations (data not shown) we have concluded that iDynoMiCS performs as expected. For details of the BM3 comparison we have to refer the reader to the *Supporting information*.

Validation of the individual-based chemostat against ODE model

We validated the individual-based chemostat submodel by simulating a multi-species community system based

on the BM3 benchmark problem. We compared steady-state biomass and solute concentrations obtained with iDynoMiCS with the deterministic solution obtained with an ODE solver implemented in MATLAB (Fig. S6). The two solutions matched well: the relative error of steady-state variables was below 2% for all variables, except when the population was particularly small (fewer than about 10 individuals in the simulation). This is to be expected when a population is composed of very few individuals, as any source of variation (such as the stochastic removal of one individual through dilution) is amplified merely because there are fewer individuals to balance out the variation. Note that this is not an artefact of the simulation, as a population consisting of few individuals in a microfluidic device or a natural system would also show such ecological drift. Increasing the system size, and therefore the number of individuals in the simulation, is one possible means to decrease variations if they are not desired, albeit at the expense of increased computation time. Further details of the validation are available in the *Supporting information*.

Example of new features in iDynoMiCS 1: the pressure field

For biofilms undergoing compaction as a result of decay or starvation processes, the biomass pressure field is a necessary model addition to allow an lbM to capture this phenomenon correctly. As an illustration, we constructed a model based on the BM3 benchmark problem, but including EPS formation ($Y_{\text{EPS}} = 0.2 \text{ g g}^{-1}$) and with increased biomass density (200 g l^{-1} for biomass and 33 g l^{-1} for EPS). After growing a biofilm for 3 days we then removed all growth and maintenance reactions from the simulation and left only EPS hydrolysis (rate $k_{\text{hyd}} = 0.013 \text{ h}^{-1}$) in order to simulate loss of biomass leading to compaction of agents. As may be seen in Fig. 3, the pressure field has a noticeable effect on the resulting biofilm thickness over 7 days of simulation. The drop in thickness of the biofilm in the simulation using pressure proceeds immediately and is linear in time, while the no-pressure simulation maintains a constant thickness for about 2 days before showing a drop in thickness. This latter drop has a shallower slope and is not caused by compaction (as in the case with the pressure field) but instead by loss of EPS particles: when hydrolysis shrinks particles too small they are removed from the simulation, thereby removing some of the biofilm's outer surface. Please see the *Supporting information* for further details of the pressure field.

Example 2: effects of continuous EPS excretion

To illustrate the benefit of using continuous rather than discrete EPS excretion, we used the same growth dynam-

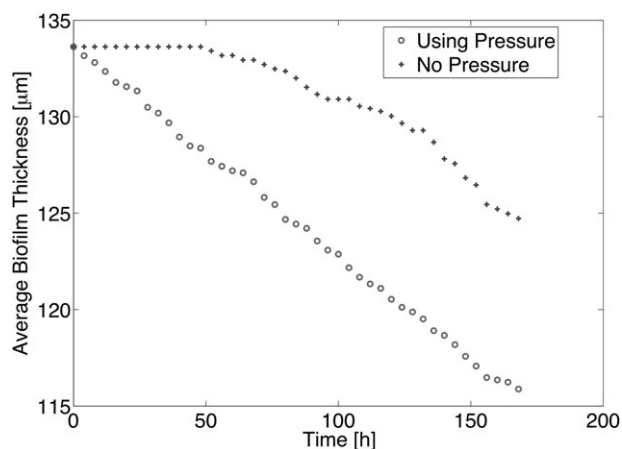


Fig. 3. Shrinking of a decaying or starving biofilm. With the new pressure field, the biofilm contracts (consolidates) without delay and at an approximately constant rate.

ics as in the previous example to simulate growth of a biofilm containing two species that are identical aside from the way in which their EPS synthesis and excretion is described. We then compared simulations for different values of the maximum EPS fraction parameter, which controls the maximum percent of an agent's volume that may be taken up by EPS before an excretion event is forced; this parameter does not affect the total amount of EPS in the biofilm but rather affects how that mass is distributed. Figure 4 shows that, for larger values of the EPS fraction parameter, the discrete-style treatment leads to a larger agent size and therefore a less well-packed biofilm; this results in an artificial height difference for the two species. The new continuous-style treatment avoids this artefact by preventing the bacterial agents from accumulating excess EPS while also removing the discontinuities that result from discrete excretion events.

In addition to alleviating possible artificial packing or height differences, we contend that a continuous-excretion treatment better captures the altruistic or spiteful effects recently ascribed to EPS production (Xavier and Foster, 2007; Nadell *et al.*, 2009). Discrete EPS excretion requires internal EPS build-up before an excretion event, and in the absence of growth the cell will no longer excrete EPS. In contrast, the continuous-excretion approach is better suited for studying EPS production as a public good because continuously excreted EPS is immediately made public.

Case study: metabolic switching for denitrification in fluctuating environments

In this case study we illustrate the utility of uncoupling individual agents from their species' metabolism so that individuals can switch metabolism because of external or

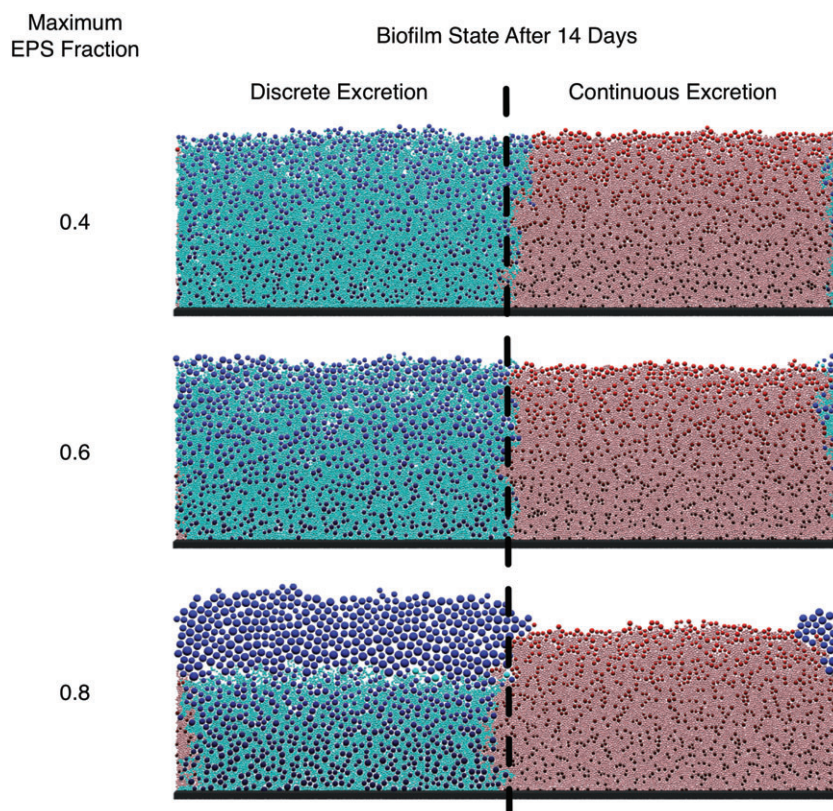


Fig. 4. Comparison of discrete- and continuous-style EPS excretion. The blue agents on the left exhibit discrete-style EPS excretion, and red agents on the right exhibit continuous-style EPS excretion. Also shown are the respective EPS particles (cyan, discrete-style; pink, continuous-style), with darker particles representing agents that are primarily composed of inert biomass. The continuous-style treatment is not affected by changes in the maximum EPS fraction parameter, but the discrete-style treatment exhibits a different structure when the EPS fraction of a capsule is allowed to be high.

internal triggers, and apply this to changing electron acceptor utilization in denitrifying bacteria. The common approach to implement such a switch mechanism is to use simple multiplicative inhibition terms such as the Monod-like term $K/(K + S)$, where the switch occurs based on local solute concentrations. With this treatment an agent may switch dominant reactions automatically as local conditions change, but in the simplest form there is an instant response to conditions; incorporation of any physiological lag periods becomes computationally more difficult. With iDynoMiCS, though, we do not need to rely on inhibition terms for activating or deactivating reaction pathways because the agents are able to activate/deactivate any of their suite of reactions, and in addition may activate/deactivate pathways based on external or internal conditions (Fig. S7). This case study illustrates an application of an externally triggered switch mechanism. More complete details of the model, results and switch algorithm are provided in the *Supporting information*.

We model a heterotrophic population growing in a bioreactor, such as in wastewater treatment applications. The heterotroph species are based on organisms that typically grow aerobically, but that may, via activation or derepression of appropriate genes, induce a denitrification pathway and use nitrate as an alternative electron acceptor when oxygen is not available or is present in low concentrations. Examples of such organisms include

Pseudomonas stutzeri, *Paracoccus denitrificans*, *Alcaligenes faecalis* and *Pseudomonas aeruginosa* (Robertson and Kuenen, 1984; Körner and Zumft, 1989; Ye *et al.*, 1995; Baumann *et al.*, 1996; Otte *et al.* 1996). We make the following assumptions based on experimental studies. Anaerobic growth of heterotrophs takes over for local oxygen concentrations below a threshold of 0.2 mg O₂/L (Ye *et al.*, 1995). After the appearance of suitable conditions, there is a delay of 1–5 h before anaerobic activity will be fully engaged (Robertson and Kuenen, 1984; Kucera *et al.*, 1990). The return to aerobic metabolism occurs instantly when oxygen is present, with anaerobic activity resuming only when the oxygen concentration has once again decreased below the threshold value (Robertson and Kuenen, 1984).

We consider three heterotrophic species that have identical growth parameters (Tables 1 and 2), but that have different denitrification pathway induction lags (1, 3 or 5 h); for simplicity we call these species Lag-1, Lag-3 and Lag-5 respectively. We also consider induction costs by comparing two cases: one in which there is an incurred maintenance cost to have a faster induction rate, and one in which there is no such cost. The rationale for assuming rapid induction to be costly is that the ability for faster adaptation of metabolic pathways would necessitate a higher rate of turnover of the cellular machinery, mainly consisting of proteins. In the no-cost case, all three

Table 1. Stoichiometric matrix for reactions in the switch case study.

| Process | Biomass | | | Solutes | | | Kinetic expression |
|-----------------------|-----------------|-------------|-------|------------------|---------------------------------------|------------------------|---|
| | Heterotrophs | EPS | Inert | COD | NO ₃ ⁻ | O ₂ | |
| Aerobic growth | $1 - Y_H^{EPS}$ | Y_H^{EPS} | | $-\frac{1}{Y_H}$ | | $-\frac{1 - Y_H}{Y_H}$ | $\mu_H^{\max} \frac{S_{COD}}{K_{COD}^H + S_{COD}} \frac{S_{O_2}}{K_{O_2}^H + S_{O_2}} X_H$ |
| Aerobic maintenance | -1 | | | | | -1 | $b_H^m \frac{S_{O_2}}{K_{O_2}^H + S_{O_2}} X_H$ |
| Anaerobic growth | $1 - Y_H^{EPS}$ | Y_H^{EPS} | | $-\frac{1}{Y_H}$ | $-\frac{1}{4.57} \frac{1 - Y_H}{Y_H}$ | | $\mu_H^{\max} \frac{S_{COD}}{K_{COD}^H + S_{COD}} \frac{S_{NO_3}}{K_{NO_3}^H + S_{NO_3}} X_H$ |
| Anaerobic maintenance | -1 | | | | $-\frac{1}{4.57}$ | | $b_H^m \frac{S_{NO_3}}{K_{NO_3}^H + S_{NO_3}} X_H$ |
| Inactivation | -1 | | 1 | | | | $b_H^i X_H$ |

species have an identical maintenance rate of 0.0133 h⁻¹, and in the cases enforcing an increasing cost with increasing rate of induction, each species has a different rate (Table 2; see *Supporting information* for details on how the rates were obtained).

We inoculated a model biofilm with an even species distribution and grew it for 10 days under different growth conditions. The basic parameters common to all cases are given in Table 3, and we compared growth under the following conditions: (i) purely aerobic (constant oxygen concentration of 4 mg l⁻¹ in the bulk compartment), (ii) purely anoxic (no oxygen in the bulk compartment) and (iii) anoxic except for regular periodic pulses that spike the bulk oxygen concentration to 0.5 mg l⁻¹, with bulk compartment outflow and consumption by the biofilm returning the oxygen concentration to zero after roughly 1 h. Figure 5 and Movies S1–S8 illustrate the effect of oxygen pulses on bulk compartment concentrations. In the case of periodic oxygen pulses we simulated pulses occurring every 2, 4, 8, 16 and 32 h. In all cases the inflow and initial bulk nitrate concentration was 4 mg-N/L. For the pulsed oxygen cases the appearance of oxygen deactivates the

anaerobic pathway and allows a brief period of aerobic growth that lasts until the added oxygen is exhausted; anaerobic growth then resumes for each species after the appropriate delay period has passed.

When switching is not costly, the fastest responding species always out-competes the others in a chemostat with fluctuating oxygen concentration, while in a constant environment all strategies are equally fit and population dynamics are entirely stochastic (see *Supporting information* for the chemostat results). Diversity of denitrifiers is therefore minimal in the fluctuating chemostat, as coexistence is not possible. In a biofilm a faster responding species will grow better under fluctuating conditions; at the highest frequencies of change (pulses every 2 or 4 h), the growth advantage of the shortest lag species is most evident. The time series plots in Fig. 6 and the final biofilm states shown in Fig. 7 illustrate these conclusions, as do Movies S9–S16. Hence, diversity in the biofilm is highest under constant aerobic or anaerobic conditions and lowest when fluctuations are most frequent. However, the weaker competitors remain in the biofilm, in contrast to the chemostat, where competitive exclusion takes place.

Table 2. Heterotroph parameter values for the switch case study.

| Parameter | Symbol | Value | Units | Source |
|--|----------------|---------------------|------------------------------------|---------|
| Maximal growth rate | μ_H^{\max} | 0.25 | h ⁻¹ | BM3 |
| Biomass yield | Y_H | 0.63 | g COD-X/g COD-S | BM3 |
| EPS yield | Y_H^{EPS} | 0.2 | g COD • g COD ⁻¹ | Assumed |
| Saturation constant for COD | K_{COD}^H | $4 \cdot 10^{-3}$ | g COD • L ⁻¹ | BM3 |
| Saturation constant for O ₂ | $K_{O_2}^H$ | $0.2 \cdot 10^{-3}$ | g O ₂ • L ⁻¹ | BM3 |
| Saturation constant for NO ₃ ⁻ | $K_{NO_3}^H$ | $0.5 \cdot 10^{-3}$ | g N • L ⁻¹ | ASM |
| Maintenance rate for Lag-5 species | b_{H1}^m | 0.0133 | h ⁻¹ | BM3 |
| Maintenance rate for Lag-3 species | b_{H2}^m | 0.0176 | h ⁻¹ | Assumed |
| Maintenance rate for Lag-1 species | b_{H3}^m | 0.0399 | h ⁻¹ | Assumed |
| Inactivation rate | b_H^i | 0.0033 | h ⁻¹ | BM3 |
| Switch threshold | $S_{O_2}^T$ | $0.2 \cdot 10^{-3}$ | g O ₂ • L ⁻¹ | YM |
| Biomass and inert density | ρ_X | 150 | g COD • L ⁻¹ | Assumed |
| EPS density | ρ_{EPS} | 30 | g COD • L ⁻¹ | Assumed |

Sources for the values were: BM3 (Noguera and Picioreanu, 2004; Rittmann *et al.*, 2004), ASM (Henze, 2000) and YM (Ye *et al.*, 1995; Matsumoto *et al.*, 2007b).

Table 3. Environmental parameter values for the switch case study.

| Parameter | Symbol | Value | Units |
|--------------------------|--------------------------|--------------------|-------------------------------------|
| Influent COD | COD_{in} | $10 \cdot 10^{-3}$ | $\text{g COD} \cdot \text{L}^{-1}$ |
| Influent NO_3^- | $\text{NO}_{3\text{in}}$ | $4 \cdot 10^{-3}$ | $\text{g N} \cdot \text{L}^{-1}$ |
| Dilution rate | D | 0.67 | h^{-1} |
| Specific area | σ_R | 80 | $\text{m}^2 \cdot \text{m}^{-3}$ |
| Erosion strength | k_{Det} | $16 \cdot 10^{-6}$ | $(\mu\text{m} \cdot \text{h})^{-1}$ |

In the more realistic case where switching is costly, there is an optimal strategy for each pulse frequency because of the trade-off between cost and response time: the slower the environment changes, the longer the optimal response time will be. In the chemostat this optimal strategy completely replaces the others: coexistence is not possible and diversity is minimal (see *Supporting information* for the chemostat results). In the biofilm, the optimal strategy does not completely replace other strategies (see Figs 6 and 7 for plots indicating this result), thus allowing for higher diversity. Note that the range of fluctuation frequencies for which the intermediate strategy is fittest is broader than for the other strategies, suggesting that this 'generalist' strategy is advantageous if the frequency of fluctuations themselves change. Intermediate pulse frequencies also allow higher diversity than in the constant environment, in contrast to the no-cost case (also seen in Figs 6 and 7).

With iDynoMiCS we are easily able to simulate growth of this system in 3 dimensions too, and when doing so we find similar results to those obtained with 2D simulations. For example, consider an inoculation of the three species that, like the 2D initial condition, creates a defined region

for each species, as illustrated in Fig. 8 and Movie S17. When this initial condition is subjected to anoxic growth conditions with oxygen pulses occurring every 4 h, the simulation outputs match the 2D results: there is roughly equal growth of all species in the early part of the simulation, but by 80 h the faster-switching species thrives at the expense of the slower-switching species, in spite of the higher cost to switch quickly. By 120 h it is clear that the faster-switching species will dominate the biofilm.

It was our goal to evaluate whether it is indeed an ecological advantage to be able to quickly induce denitrification under low oxygen concentrations as has been postulated (Robertson and Kuenen, 1984), and we find that when there is no cost to fast induction the advantage of this strategy is clear. However, when there is a cost to faster induction a trade-off results, which renders the optimal growth strategy dependent on the environment and competing species, similar to the trade-off between rate- and yield-based growth strategies (Kreft, 2004). Traditional inhibition-based reaction kinetics are not ideal for use in this type of study because those equations show instant responses and would thus require some workaround in order to capture the on/off switching with lags. With iDynoMiCS, though, we could incorporate the induction lags into the model directly, allowing individual agents to activate or deactivate reaction pathways in response to local conditions.

Conclusion

iDynoMiCS is a new computational tool intended to lower the barrier to biofilm modelling by non-programmers, but

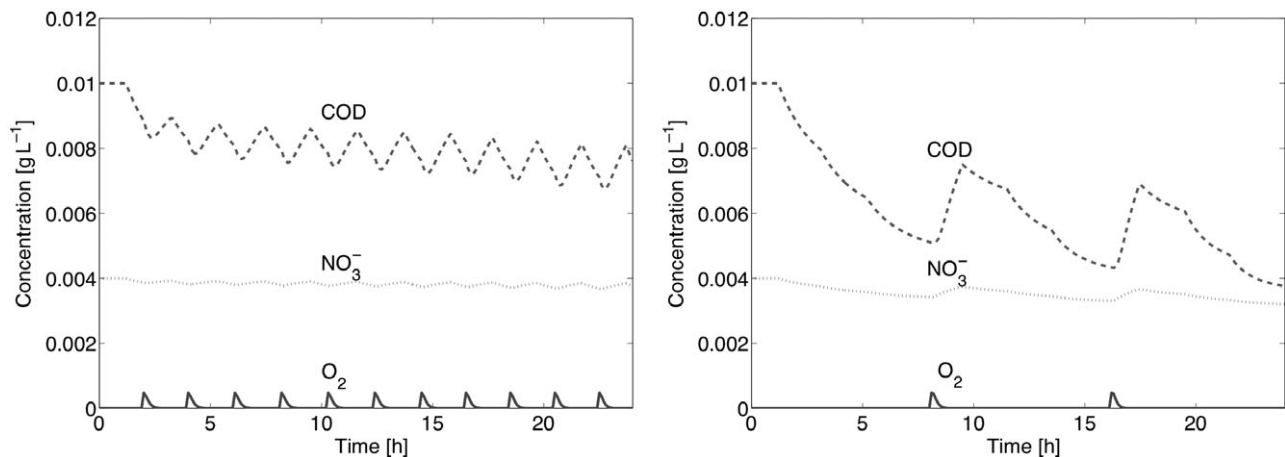
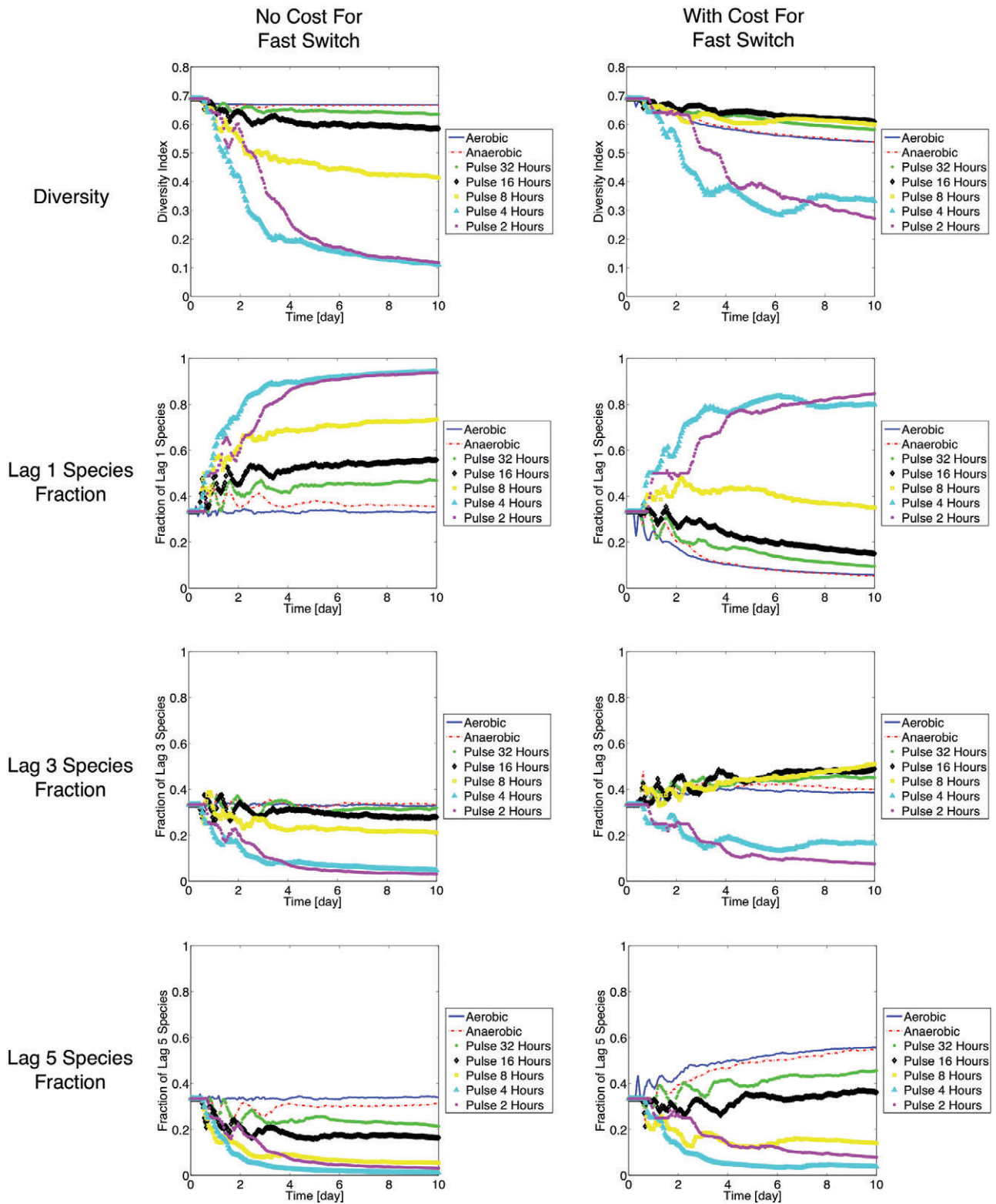


Fig. 5. Bulk reactor concentrations when oxygen is pulsed every 2 (left) and 8 (right) hours. Shown is an example 24 h period of bulk concentrations during oxygen pulses. The oxygen concentration quickly drops to zero after rising to $0.5 \text{ mg O}_2/\text{L}$ during a pulse, and the pulse affects both COD and nitrate concentrations in the bulk because of activation of the aerobic growth pathway. After oxygen is depleted, the COD and nitrate concentrations begin to rise until the anaerobic pathway is re-induced by the Lag-1 species, at which point the concentrations begin to drop once again. When pulses occur every 2 h this is the only species that is able to induce its anaerobic pathway, but when pulses occur every 8 h there are additional drops in the COD and nitrate concentrations as the Lag-3 and Lag-5 species also induce their anaerobic pathways.



iDynoMiCS also introduces several advances to biofilm modelling techniques and addresses limitations in previous models. Foremost among these advances are the inclusion of a pressure field to model biomass spreading

or consolidation, improvements to the treatment of EPS (non-growth-dependent excretion and use of smaller particles), the ability to easily model an unstructured chemostat environment and, perhaps most importantly, the

Fig. 6. Species diversity and survival after 10 days of growth as dependent on environmental conditions and on metabolic costs. The Diversity Index was calculated via:

$$D_{\text{Diversity}} \equiv 1 - \frac{\sum_k n_k (n_k - 1)}{N_T (N_T - 1)}$$

where n_k is the number of individuals of species k and N_T is the total number of individuals. An index of 1 represents complete diversity (each individual is a unique species), while an index of 0 represents complete homogeneity (only one species present). For the calculation of this index we included only bacterial agents and excluded EPS agents. Similarly, the fraction of a given species at each point in time is calculated as n_k/N_T . When there is no cost for fast induction of the anaerobic pathway, species diversity decreases with an increasingly fluctuating environment. But when there is a metabolic cost to fast induction, intermediate-rate fluctuations lead to the highest diversity. See Fig. 7 for the biofilm structures obtained after 10 days.

ability for individuals of a species to behave in a truly individual manner as metabolic reactions are no longer hard-wired into the repertoire of the individual. The new features in iDynoMiCS have already proven fruitful in the case study of metabolic switching triggered by external oxygen concentrations. For the case of a trade-off between rate of response to environmental change and

cost of metabolic reorganization, there is an optimal lag time that relates to the frequency of environmental change. This explains how the existence of different regulatory strategies in denitrifying bacteria can be maintained. We found that chemostats show competitive exclusion but biofilms maintain a diverse community, and that this diversity is highest under fluctuating conditions.

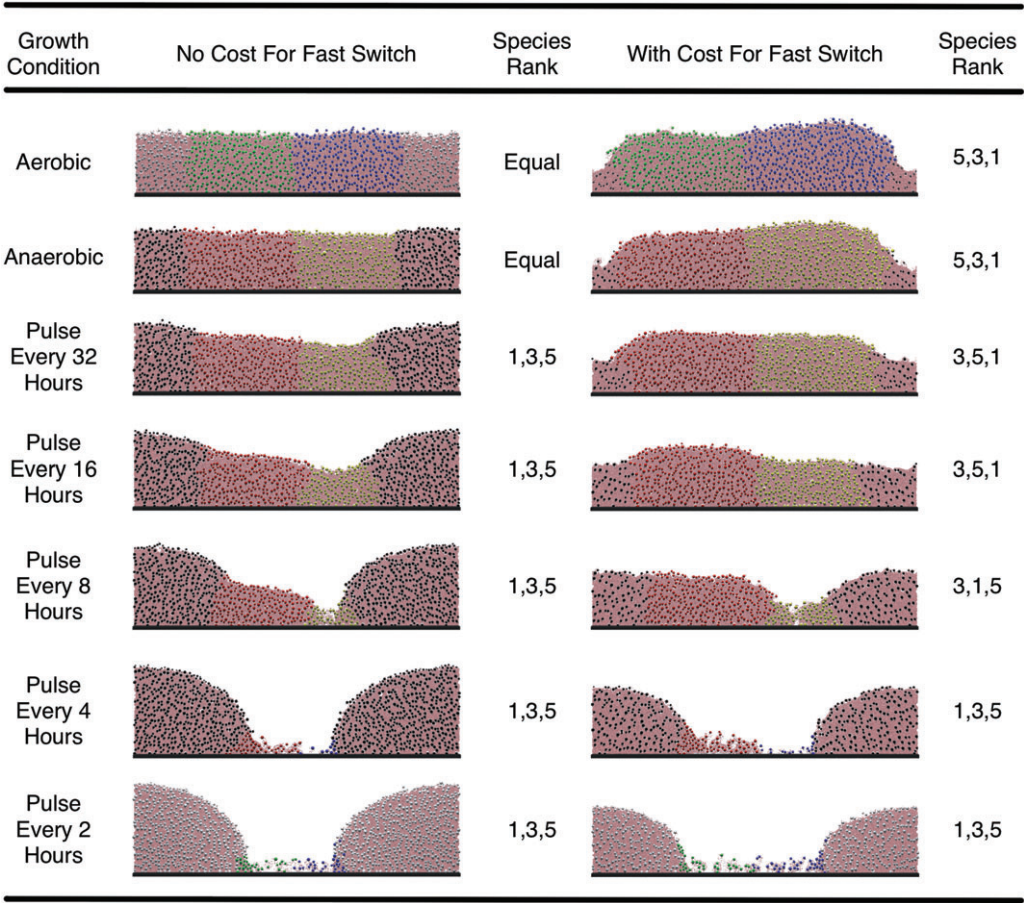


Fig. 7. Comparison of biofilm composition after 10 days for different growth conditions. The colours used to represent the on/off states for the species types are: black/white for Lag-1, red/green for Lag-3 and yellow/blue for Lag-5. The smaller pink agents are EPS particles. All cases were inoculated with the substratum divided into three equal parts, each covered by a different species. Species ranks are by total number of agents of each species. When there is no cost for fast induction of the anaerobic pathway, a fluctuating environment selects for the fastest-responding (lowest-lag) species. When the cost of induction increases with increasing rate of response, the slowest-responding species dominates at constant conditions and the fastest-responding species dominates at higher fluctuating frequency, while the intermediate species dominates at intermediate conditions.

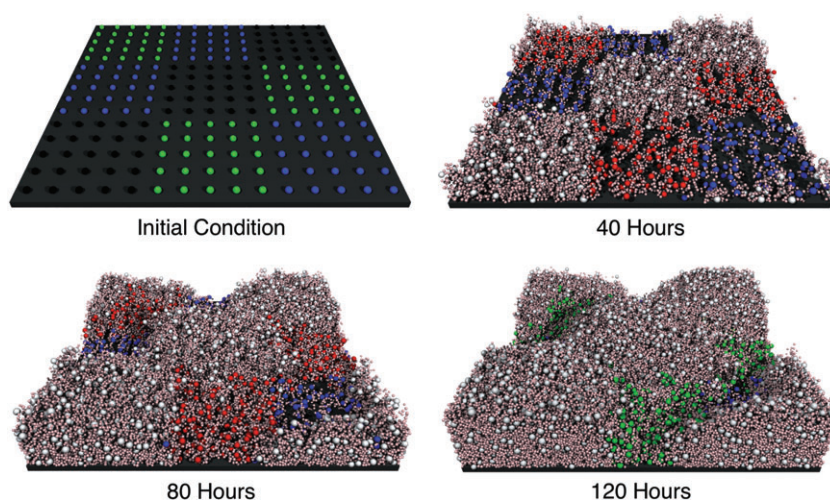


Fig. 8. Example biofilm structures from 3D simulations (with-cost case). Time evolution of a biofilm growing under anoxic conditions with oxygen pulses occurring every 4 h. Agent colours are black/white for Lag-1, red/green for Lag-3, yellow/blue for Lag-5, and pink for EPS as in Fig. 7. As in the 2D simulations, the faster-switching species tend to outgrow the other species in spite of the cost for being a faster switcher.

We suggest that this higher diversity may buffer the microbial community in a biofilm against periodic but also unpredictable changes. The iDynoMiCS platform has also been used in a study of plasmid spread in biofilms (Merkey *et al.*, 2011), and work is already underway to extend the iDynoMiCS framework to include additional microbial organisms (such as planktonic species) and new growth geometries. The modular nature of iDynoMiCS makes such extensions easy and natural, which was one of the original goals in developing iDynoMiCS. Included in the *Supporting information* are details describing how to obtain iDynoMiCS.

Acknowledgements

Work at DTU by BFS, LAL and BVM was supported by a Marie Curie Excellence Grant (MEXT-CT-2005-024004, RaMAda) to BFS. AD acknowledges financial support by the Helmholtz Gemeinschaft and the DFG-sponsored International Research Training Group 'Pseudomonas: Pathogenicity and Biotechnology'. We thank Chinmay Kanchi and Edward M Miles (Birmingham) for administrative support of the code development and enhancements to launch the programme and repeat runs automatically. JUK acknowledges financial support by the Deutsche Forschungsgemeinschaft (DFG) through the collaborative research centre on 'Singular Phenomena and Scaling in Mathematical Models' (SFB 611).

References

- Alpkvist, E., and Klapper, I. (2007a) Description of mechanical response including detachment using a novel particle model of biofilm/flow interaction. *Water Sci Technol* **55**: 265–273.
- Alpkvist, E., and Klapper, I. (2007b) A Multidimensional Multispecies Continuum Model for Heterogeneous Biofilm Development. *Bull Math Biol* **69**: 765–789.
- Alpkvist, E., Picioreanu, C., van Loosdrecht, M.C.M., and Heyden, A. (2006) Three-Dimensional Biofilm Model With

- Individual Cells and Continuum EPS Matrix. *Biotechnol Bioeng* **94**: 961–979.
- Balagaddé, F.K., You, L., Hansen, C.L., Arnold, F.H., and Quake, S.R. (2005) Long-term monitoring of bacteria undergoing programmed population control in a microchemostat. *Science* **309**: 137–140.
- Batstone, D.J., Picioreanu, C., and van Loosdrecht, M.C.M. (2006) Multidimensional modelling to investigate interspecies hydrogen transfer in anaerobic biofilms. *Water Res* **40**: 3099–3108.
- Baumann, B., Snozzi, M., Zehnder, A.J., and Van Der Meer, J.R. (1996) Dynamics of denitrification activity of *Paracoccus denitrificans* in continuous culture during aerobic-anaerobic changes. *J Bacteriol* **178**: 4367.
- Bishop, P.L., and Yu, T. (1999) A microelectrode study of redox potential change in biofilms. *Water Sci Technol* **39**: 179–185.
- Boles, B.R., Thoendel, M., and Singh, P.K. (2004) Self-generated diversity produces 'insurance effects' in biofilm communities. *Proc Natl Acad Sci USA* **101**: 16630–16635.
- Brandt, A. (1977) Multi-level adaptive solutions to boundary-value problems. *Math Comput* **31**: 333–390.
- Characklis, W.G., and Marshall, K.C. (1990) *Biofilms*. New York, NY, USA: John Wiley & Sons.
- Dockery, J., and Klapper, I. (2001) Finger formation in biofilm layers. *SIAM J Appl Math* **62**: 853–869.
- Downing, L.S., and Nerenberg, R. (2008) Effect of oxygen gradients on the activity and microbial community structure of a nitrifying, membrane-aerated biofilm. *Biotechnol Bioeng* **101**: 1193–1204.
- Duddu, R., Chopp, D.L., and Moran, B. (2009) A two-dimensional continuum model of biofilm growth incorporating fluid flow and shear stress based detachment. *Biotechnol Bioeng* **103**: 92–104.
- Eberl, H., Parker, D.F., and van Loosdrecht, M.C.M. (2001) A new deterministic spatio-temporal continuum model for biofilm development. *J Theor Med* **3**: 161–175.
- Ebrahimi, S., Picioreanu, C., Kleerebezem, R., Heijnen, J.J., and van Loosdrecht, M.C.M. (2005) Rate based modeling of a sulfite reduction bioreactor. *AIChE J* **51**: 1429–1439.
- Freter, R., Freter, R.R., and Brickner, H. (1983) Experimental

- and mathematical models of *Escherichia coli* plasmid transfer in vitro and in vivo. *Infect Immun* **39**: 60–84.
- Gear, C.W. (1971) *Numerical Initial Value Problems in Ordinary Differential Equations*. Upper Saddle River, NJ, USA: Prentice Hall.
- Gingold, R.A., and Monaghan, J.J. (1977) Smoothed particle hydrodynamics- theory and application to non-spherical stars. *Mon Not R Astron Soc* **181**: 375–389.
- Grimm, V., Berger, U., Bastiansen, F., Eliassen, S., Ginot, V., Giske, J., *et al.* (2006) A standard protocol for describing individual-based and agent-based models. *Ecol Modell* **198**: 115–126.
- Hellweger, F.L., and Bucci, V. (2008) A bunch of tiny individuals – individual-based modeling for microbes. *Ecol Modell* **220**: 8–22.
- Henze, M. (2000) *Activated Sludge Models ASM1, ASM2, Asm2d and ASM3*. London, UK: IWA Publishing.
- Heydorn, A., Ersbøll, B.K., Hentzer, M., Parsek, M.R., Givskov, M., and Molin, S. (2000) Experimental reproducibility in flow-chamber biofilms. *Microbiology* **146**: 2409–2415.
- Kaern, M., Elston, T.C., Blake, W.J., and Collins, J.J. (2005) Stochasticity in gene expression: from theories to phenotypes. *Nat Rev Genet* **6**: 451–464.
- Klapper, I., Rupp, C.J., Cargo, R., Purvedorj, B., and Stoodley, P. (2002) Viscoelastic fluid description of bacterial biofilm material properties. *Biotechnol Bioeng* **80**: 289–296.
- Körner, H., and Zumft, W.G. (1989) Expression of denitrification enzymes in response to the dissolved oxygen level and respiratory substrate in continuous culture of *Pseudomonas stutzeri*. *Appl Environ Microbiol* **55**: 1670.
- Kreft, J.-U. (2004) Biofilms promote altruism. *Microbiology* **150**: 2751–2760.
- Kreft, J.-U., and Wimpenny, J.W.T. (2001) Effect of EPS on biofilm structure and function as revealed by an individual-based model of biofilm growth. *Water Sci Technol* **43**: 135–141.
- Kreft, J.-U., Booth, G., and Wimpenny, J.W.T. (1998) BacSim, a simulator for individual-based modelling of bacterial colony growth. *Microbiology* **144**: 3275–3287.
- Kreft, J.-U., Picioreanu, C., Wimpenny, J.W.T., and van Loosdrecht, M.C.M. (2001) Individual-based modelling of biofilms. *Microbiology* **147**: 2897–2912.
- Kucera, I., Matchová, I., and Dadák, V. (1990) Respiratory rate as a regulatory factor in the biosynthesis of the denitrification pathway of the bacterium *Paracoccus denitrificans*. *Biocatal Biotransformation* **4**: 29–37.
- Laspidou, C.S., and Rittmann, B.E. (2004a) Evaluating trends in biofilm density using the UMCCA model. *Water Res* **38**: 3362–3372.
- Laspidou, C.S., and Rittmann, B.E. (2004b) Modeling the development of biofilm density including active bacteria, inert biomass, and extracellular polymeric substances. *Water Res* **38**: 3349–3361.
- Lawrence, J.R., Korber, D.R., Hoyle, B.D., Costerton, J.W., and Caldwell, D.E. (1991) Optical Sectioning of Microbial Biofilms. *J Bacteriol* **173**: 6558–6567.
- Mabrouk, M., Deffuant, G., Tolker-Nielsen, T., and Lobry, C. (2010) Bacteria can form interconnected microcolonies when a self-excreted product reduces their surface motility: evidence from individual-based model simulations. *Theory Biosci* **129**: 1–13.
- Matsumoto, S., Terada, A., Aoi, Y., Tsuneda, S., Alpkvist, E., and Picioreanu, C. (2007a) Experimental and simulation analysis of community structure of nitrifying bacteria in a membrane-aerated biofilm. *Water Sci Technol* **55**: 283–290.
- Matsumoto, S., Terada, A., and Tsuneda, S. (2007b) Modeling of membrane-aerated biofilm: effects of C/N ratio, biofilm thickness and surface loading of oxygen on feasibility of simultaneous nitrification and denitrification. *Biochem Eng J* **37**: 98–107.
- Matsumoto, S., Katoku, M., Saeki, G., Terada, A., Aoi, Y., Tsuneda, S., *et al.* (2010) Microbial community structure in autotrophic nitrifying granules characterized by experimental and simulation analyses. *Environ Microbiol* **12**: 192–206.
- Merkey, B.V., Rittmann, B.E., and Chopp, D.L. (2009) Modeling how soluble microbial products (smp) support heterotrophic bacteria in autotroph-based biofilms. *J Theor Biol* **259**: 670–683.
- Merkey, B.V., Lardon, L., Seoane, J.M., Kreft, J.-U., and Smets, B.F. (2011) Growth dependence of conjugation explains limited plasmid invasion in biofilms: an individual-based modeling study. *Environ Microbiol* (in press).
- Nadell, C.D., Xavier, J.B., and Foster, K.R. (2009) The sociobiology of biofilms. *FEMS Microbiol Rev* **33**: 206–224.
- Noguera, D., and Picioreanu, C. (2004) Results from the multi-species Benchmark Problem 3 (BM3) using two-dimensional models. *Water Sci Technol* **49**: 169–176.
- Otte, S., Grobbs, N., Robertson, L., Jetten, M., and Kuenen, J. (1996) Nitrous oxide production by *Alcaligenes faecalis* under transient and dynamic aerobic and anaerobic conditions. *Appl Environ Microbiol* **62**: 2421.
- Picioreanu, C., van Loosdrecht, M.C.M., and Heijnen, J.J. (1999) Discrete-differential modelling of biofilm structure. *Water Sci Technol* **39**: 115–122.
- Picioreanu, C., van Loosdrecht, M.C.M., and Heijnen, J.J. (2001) Two-dimensional model of biofilm detachment caused by internal stress from liquid flow. *Biotechnol Bioeng* **72**: 205–218.
- Picioreanu, C., Kreft, J.-U., and van Loosdrecht, M.C.M. (2004a) Particle-based multidimensional multispecies biofilm model. *Appl Environ Microbiol* **70**: 3024–3040.
- Picioreanu, C., Xavier, J., and van Loosdrecht, M.C.M. (2004b) Advances in mathematical modeling of biofilm structure. *Biofilms* **1**: 1–13.
- Picioreanu, C., Batstone, D.J., and van Loosdrecht, M.C.M. (2005) Multidimensional modelling of anaerobic granules. *Water Sci Technol* **52**: 501–507.
- Picioreanu, C., Kreft, J.U., Klausen, M., Haagensen, J.A.J., Tolker-Nielsen, T., and Molin, S. (2007) Microbial motility involvement in biofilm structure formation – a 3d modelling study. *Water Sci Technol* **55**: 337–343.
- Reichert, P. (1994) Aquasim – a tool for simulation and data-analysis of aquatic systems. *Water Sci Technol* **30**: 21–30.
- Rittmann, B.E., and McCarty, P.L. (2001) *Environmental Biotechnology: Principles and Applications*. New York, NY, USA: McGraw-Hill.

- Rittmann, B.E., and Manem, J.A. (1992) Development and experimental evaluation of a steady-state, multispecies biofilm model. *Biotechnol Bioeng* **39**: 914–922.
- Rittmann, B.E., Schwartz, A.O., Eberl, H., Morgenroth, E., Pérez, J., van Loosdrecht, M.C.M., and Wanner, O. (2004) Results from the multi-species Benchmark Problem 3 (BM3) using one-dimensional models. *Water Sci Technol* **49**: 163–168.
- Robertson, L.A., and Kuenen, J.G. (1984) Aerobic denitrification – old wine in new bottles? *Antonie Van Leeuwenhoek* **50**: 525–544.
- Shampine, L.F. (1982) Implementation of rosenbrock methods. *ACM Trans Math Softw* **8**: 93–113.
- Shampine, L.F., and Reichelt, M.W. (1997) The matlab ODE suite. *SIAM J Sci Comput* **18**: 1–22.
- Stewart, P.S. (2003) Diffusion in biofilms. *J Bacteriol* **185**: 1485.
- Stewart, P.S., and Franklin, M.J. (2008) Physiological heterogeneity in biofilms. *Nat Rev Microbiol* **6**: 199.
- Stoodley, P., Sauer, K., Davies, D.G., and Costerton, J.W. (2002) Biofilms as complex differentiated communities. *Annu Rev Microbiol* **56**: 187–209.
- Wanner, O., and Gujer, W. (1986) A multispecies biofilm model. *Biotechnol Bioeng* **28**: 314–328.
- Wanner, O., and Reichert, P. (1996) Mathematical modeling of mixed-culture biofilms. *Biotechnol Bioeng* **49**: 172–184.
- Wanner, O., Eberl, H.J., van Loosdrecht, M.C.M., Morgenroth, E., Noguera, D.R., Picioreanu, C., and Rittmann, B.E. (2006) *Mathematical Modeling of Biofilms*. London, UK: IWA Publishing.
- Watnick, P., and Kolter, R. (2000) Biofilm, city of microbes. *J Bacteriol* **182**: 2675–2679.
- Xavier, J., and Foster, K.R. (2007) Cooperation and conflict in microbial biofilms. *Proc Natl Acad Sci USA* **104**: 876–881.
- Xavier, J., White, D.C., and Almeida, J.S. (2003) Automated biofilm morphology quantification from confocal laser scanning microscopy imaging. *Water Sci Technol* **47**: 31–37.
- Xavier, J., Picioreanu, C., and van Loosdrecht, M.C.M. (2005a) A framework for multidimensional modelling of activity and structure of multispecies biofilms. *Environ Microbiol* **7**: 1085–1103.
- Xavier, J., Picioreanu, C., and van Loosdrecht, M.C.M. (2005b) A general description of detachment for multidimensional modelling of biofilms. *Biotechnol Bioeng* **91**: 651–669.
- Xavier, J.B., Picioreanu, C., Rani, S.A., van Loosdrecht, M.C.M., and Stewart, P.S. (2005c) Biofilm-control strategies based on enzymic disruption of the extracellular polymeric substance matrix – a modelling study. *Microbiology* **151**: 3817–3832.
- Xavier, J., de Kreuk, M.K., Picioreanu, C., and van Loosdrecht, M.C.M. (2007) Multi-scale individual-based model of microbial and bioconversion dynamics in aerobic granular sludge. *Environ Sci Technol* **41**: 6410–6417.
- Ye, R.W., Haas, D., Ka, J.O., Krishnapillai, V., Zimmermann, A., Baird, C., and Tiedje, J.M. (1995) Anaerobic activation of the entire denitrification pathway in *Pseudomonas aeruginosa* requires Anr, an analog of Fnr. *J Bacteriol* **177**: 3606.

Supporting information

Additional Supporting Information may be found in the online version of this article:

Fig. S1. Agent behaviour at boundaries.

Fig. S2. Pressure field contours.

Fig. S3. Cell division.

Fig. S4. Shoving of neighbouring cells is triggered if there is an overlap between them.

Fig. S5. Example of isolines of erosion time computed with the fast marching algorithm.

Fig. S6. Comparison of simulations of the stochastic chemostat model using iDynoMiCS with simulations of the deterministic ODE model using the ODE solver ode23s of Matlab.

Fig. S7. Metabolic switch algorithm.

Table S1. Simple example reaction description and stoichiometric matrix.

Table S2. Reactions matrix for BM3 problem (Rittmann et al., 2004).

Table S3. Parameter values for BM3 problem (Rittmann et al., 2004).

Table S4. Environmental conditions for BM3 problem (Rittmann et al., 2004).

Table S5. Results of BM3 simulations.

Table S6. Chemostat results for the metabolic switch case study.

Algorithm S1. When a chemostat is being simulated, step 1 is simplified due to the spatial homogeneity but the time resolution is increased, steps 2, 3c, and 3d are skipped, and step 4 is replaced by stochastic agent dilution.

Movies S1–S8. These movies illustrate biofilm growth *without cost* for fast switching.

Movie S1. Growth under aerobic conditions.

Movie S2. Growth under anaerobic conditions.

Movie S3. Growth under anaerobic conditions interrupted by an oxygen pulse every 32 hours.

Movie S4. Growth under anaerobic conditions interrupted by an oxygen pulse every 16 hours.

Movie S5. Growth under anaerobic conditions interrupted by an oxygen pulse every 8 hours.

Movie S6. Growth under anaerobic conditions interrupted by an oxygen pulse every 4 hours.

Movie S7. Growth under anaerobic conditions interrupted by an oxygen pulse every 2 hours.

Movie S8. Growth under anaerobic conditions interrupted by randomly-occurring oxygen pulses.

Movies S9–S16. These movies illustrate biofilm growth *when there is a cost* for fast switching.

Movie S9. Growth under aerobic conditions.

Movie S10. Growth under anaerobic conditions.

Movie S11. Growth under anaerobic conditions interrupted by an oxygen pulse every 32 hours.

Movie S12. Growth under anaerobic conditions interrupted by an oxygen pulse every 16 hours.

Movie S13. Growth under anaerobic conditions interrupted by an oxygen pulse every 8 hours.

Movie S14. Growth under anaerobic conditions interrupted by an oxygen pulse every 4 hours.

Movie S15. Growth under anaerobic conditions interrupted by an oxygen pulse every 2 hours.

Movie S16. Growth under anaerobic conditions interrupted by randomly-occurring oxygen pulses.

Movie S17. This movie illustrates a 3D simulation of biofilm growth under anaerobic conditions interrupted by an oxygen pulse every 4 hours when there is a cost for fast switching.

Please note: Wiley-Blackwell are not responsible for the content or functionality of any supporting materials supplied by the authors. Any queries (other than missing material) should be directed to the corresponding author for the article.